3D EIT system for breast cancer detection

V Cherepenin[1], A Karpov[2], A Korjenevsky[1], V Kornienko[1], A Mazaletskaya[3] D Mazourov[4] and D Meister[5]

[1]Institute of Radio-Engineering and Electronics of Russian Academy of Sciences, Moscow, Russia
[2]Clinical Hospital No 9, Yaroslavl, Russia
[3]Yaroslavl State University, Russia
[4]Regional Oncological Hospital, Yaroslavl, Russia
[5]Technology Commercialization International, Inc., Albuquerque, NM, USA

Classification numbers: 87.63.-d, 87.63.Pn

Keywords: electrical impedance tomography, breast cancer detection, bio-impedance, medical imaging.

[1] E-mail: korjenevsky@cplire.ru
[3] E-mail: almaz@yars.free.net
[5] E-mail: tcintl@nm.net

Abstract. A medical device, which allows imaging 3d conductivity distribution in the subsurface areas using the EIT approach, has been developed and tested. The purpose of the new system is the early detection and preliminary diagnosis of the breast tumours. Design of the measuring system and software are described. Results of clinical evaluation of the system are presented. EIT images of healthy and cancerous breasts are given and discussed. The evaluated system distinguishably visualises various states of the breast and can be applied to breast cancer detection.

Introduction

It is known that electrical conductivity of many tumours, in particular the malignant tumours of the mammary gland, significantly differs from the conductivity of surrounding sound tissues (Rigaud *et al* 1996). This fact provides an efficient, safe and inexpensive way to detect and localise such tumours. The electrical impedance tomography (EIT) enables visualisation of the spatial distribution of conductivity in the human body and several research groups work on EIT systems for breast imaging (see, for example, Tunstall *et al* 1998, Wtorek *et al* 1999). Application of this method in breast cancer detection requires special design of the measuring system and image reconstruction algorithm. The imaging of a three-dimensional distribution of conductivity is required. The resolution of the EIT system falls significantly with increasing distance from measuring electrodes. The traditional EIT measurement schemes are inefficient in mammography due to this. A large number of electrodes, required to provide acceptable resolution of the system, leads to enormous increases in computation time for image reconstruction.

The prototype of the breast cancer detection device (BCDD), providing conductivity visualisation of subsurface areas, suitable for carrying out clinical researches, has been developed in the Institute of Radio-Engineering and Electronics of Russian Academy of Sciences with the support of Technology Commercialization International, Inc. (USA). The 3-D EIT system for breast cancer detection uses measurement and three-dimensional (3-D) reconstruction of the conductivity distribution in biological tissues for clinical diagnoses. It consists of a compact array of electrodes positioned over the tissue being measured, two additional electrodes spaced apart from the array of electrodes, a source of alternating (AC) current, a means to measure potential difference, and computing means to reconstruct and visualise the resulting conductivity distribution as stack of tomographic images.

A comparative analysis of breast electrical impedance images obtained with the new system for normal and cancerous tissues is also provided in this paper.

Materials and methods

2.1. Measuring system

The measurements are carried out using 256 electrodes, which are arranged in square matrix with 12-cm side. The electrodes are placed on the rigid plane, each electrode protrudes from the plane. During an examination, the plane of electrodes is pressed against the breast, flattening it toward the chest, increasing the number of electrodes having contact with the body and decreasing the thickness of the tissue layer to be measured. The main parts of the 3-D EIT system include an output multiplexer is connected to the electrode array and is the means by which the alternating current (AC) source is connected to one of the electrodes in the array. An input multiplexer serves to connect one of the non-activated or rest electrodes of the array to a potential difference-measuring unit. A microprocessor within the 3-D EIT system and the computer, connected via cables determine which electrode is activated and which of the rest electrodes is being measured at any given time. Two single remote electrodes are attached to the extremities of the patient. One remote electrode is connected directly to a safe AC source (0.2ma, at 10kHz, whereas the maximum allowable safe level is 1.0 ma, at 10kHz). The other remote electrode is connected directly to a potential difference detector. The 3-D EIT system

operation is controlled by a microprocessor/computer means. It gets inputs from the potential difference detector and the threshold detector and outputs to the two multiplexers, the potential difference detector, and the AC source.

In contrast with standard EIT measurement strategy, in the described 3-D EIT system, the output multiplexer switches a single lead from the AC source to activate a single electrode in the electrode array at a time, instead of activating pairs of electrodes. The second activated electrode is the remote electrode that is always on. The same is true for the input multiplexer. The potential difference detector measures the difference between the selected array electrode and the remote rest electrode. For a given input electrode, the output multiplexer sequences through all the other electrodes in the array while the potential difference detector makes its measurements. Then the input electrode is switched and the output multiplexer sequence repeated. Switching a single lead at a time reduces the spurious couplings arising from channel-to-channel penetration of signals in the multiplexer. It also simplifies the device and reduces its cost. The distance of the singular electrodes from the electrode array allows one to assume that the unperturbed equipotential surfaces of electric field are spherical in the examination area. It simplifies and speeds up the conductivity reconstruction calculations.

The current injection and voltage measurement circuitry is similar to the one in our electrical impedance tomograph with static imaging (Cherepenin *et al* 1995, Korjenevsky *et al* 1997). In the current source the digital-to-analog converter provides the input signal for the voltage-to-current converter consisting of 3 operational amplifiers. In the potential difference-measuring unit the analogue synchronous detector and switchable integrator convert real part of input AC potential differences to DC before analogue to digital conversion. The 16-bit analog-to-digital converter is applied in voltage measurements. Fast-response circuit for galvanic potential compensation enables reliable measurements with stainless steel electrodes. The full measurement cycle (65280 voltage measurements) takes less than 20 s. Since part of the electrodes on the plane can be out of contact with patient's body, the measuring system is provided with a voltage threshold detector connected to the current source for checking the quality of contacts. Information from this circuit is used during image reconstruction. Figure 1 illustrates physical configuration of the system and measurement procedure.

2.2. Reconstruction software

The method of back projection is one of the fastest in electrical impedance tomography reconstruction and seems most suitable in 3-D applications, when the number of electrodes is so large as 256 and the time required for calculations become critical. The 3-D EIT system uses a method of weighted back projection along equipotential surfaces of the electric field to reconstruct the 3-D conductivity distribution and provides visualisation of several cross-sections ("slices"), which are parallel to the electrodes array, see Figure 2.

It is assumed that in the case where the electric current is injected through one of the electrodes in a planar array and the remote common electrode, equipotential surfaces near the array are spherical. The procedure of back projection is reduced to the following. For some point with coordinates (x,y,z) inside the object under visualization, the distance is determined between this point and the injecting electrode of the array. This distance is equal to the radius r of the equipotential surface containing the point where the conductivity is reconstructed. Knowing this radius, it is possible to determine the line of intersection of the equipotential surface with the surface on which the electrodes are arranged. When the electrodes are arranged on the plane, given by equation $z=0$, this line is the circle lying in the (x, y) plane having its center at the point where the injecting electrode is located, and having radius r. Conductivity S (in arbitrary units) at the chosen point is calculated according to the equation:

$$S(x,y,z) = 1 + W_1(z) \sum_i \frac{1}{\int_{L(x,y,z,i)} W_2(l)\,dl} \int_{L(x,y,z,i)} W_2(l)\,(E_r(l) - E_m(l))/E_r(l)\,dl \quad ,$$

where i is the number of the injecting electrode, $L(x,y,z,i)$ - is the line of intersection of the equipotential surface with the surface on which the electrodes are arranged (circle with radius r). The components of the electric field vector E_m are first calculated at the nodes of the grid between the electrodes as the potential differences between adjacent electrodes in the x and y directions. Then these components are linearly interpolated to the current point of integration on the line L and the magnitude of this vector E_m is calculated. The reference intensity of the electric field E_r corresponds to a homogeneous medium and is calculated numerically using the reference data set synthesis technique (Korjenevsky 1995) to improve static imaging.. Weighting coefficient $W_1(z)$ corrects the decrease of sensitivity with depth as $W_1 = (z+\alpha)/(z+\beta), \alpha << \beta$.

The weighting coefficient W_2 provides a relatively greater contribution to the calculated conductivity of those points on line L, which are located closer to the point at which the conductivity is reconstructed. The 3-D EIT system uses the equation $W_2 = 1/R^4 = 1/\left((x-x_l)^2 + (y-y_l)^2 + z^2\right)^2$, where R is the distance between the point where the conductivity is reconstructed and the current point on the line along which integration is being carried out; the index l refers to the coordinates of this point.

Whenever it is difficult to obtain sufficient contact of all the electrodes with the patient's body, then the output voltage of the threshold detector is used to determine whether the electrode being measured at any particular moment has sufficient contact with the body. The values of the potential differences measured from electrodes that have insufficient body contact cannot be used directly in the process of conductivity reconstruction. Instead, values of potential differences calculated based on a homogeneous conductivity distribution are used.

The resulting electrical impedance image represents tissue conductivity in gray scale from dark to light, from low conductivity to high respectively. The time that is required for the reconstruction of conductivity distribution in 7 cross-sections (with 8-mm depth step) is less than 1 min with Pentium II 300 MHz processor.

2.3. Testing of the system

The device was tested on the water tank and on the volunteers (the male breast, which is not so complicated an object as the female breast, was investigated in the first trials). The tank measurements were carried out with the device placed horizontally above open surface of the saline. The tank, filled with 1-% by weight concentration saline, had 10-cm depth and square 30x30-cm cross-section. The remote electrodes were placed on the bottom of the tank at its corners. The tests with tank have demonstrated the goodness of visualisation with depth Z from the electrodes of the order of 5 cm. The example of tank imaging is shown on Figure 3. The 5-cm diameter and 9 cm height cylindrical glass was immersed vertically to the saline. The distance between the electrodes and top of the glass was approximately 1 cm. As expected, the cross-section of cylinder is the circle at any depth. The thickness of circles increases with depth due to decreasing of device resolution. The decrease of resolution with distance from the electrodes is common problem in all EIT system including 3-D of course. Other tank measurements were performed with small test objects in order to estimate resolution and sensitivity of the system. In such tests the device clearly imaged an 8-mm ball made from aluminium foil on the 2-cm depth.

An example of in vivo imaging is demonstrated on the Figure 4. The measurements were made on the male breast. The volunteer was 40 years old with normal constitution and without excessive fat. Many electrodes were not in contact with the body. The bad contact areas appear as white fields accompanied with dark contours artefacts on the periphery of the images. Nevertheless the central parts of the images corresponding to the 3 depth levels demonstrate good correlation with real anatomic structures. The nipple area is visible as high-conductive spot on the surface image (Figure 4a) but become low conductive at dipper layers. The ribs become visible at 1-cm depth cross-section. The muscle tissues looks rather homogeneous in the captured area.

3. Clinical measurements

A total of 21 women were examined. Patients were chosen with tumour localisation in one breast. The size of tumours determined by means of x-ray mammography was from 1.5 to 5 cm. Intact breast was supposed conventionally healthy. Examinations were made in two positions – lying and standing. The obtained 84 electrical impedance mammograms (EIM) - images of two breast in two positions for each patient were sorted onto groups. Group 1 consists of 42 EIM of intact breast; group 2 - 42 EIM of breast with clinical diagnosis “breast cancer”. After examination, group 2 was divided into additional group 3 - 16 EIM without focal alterations on EIM and group 4 - 26 EIM with focal alterations. The focal alteration is palpable tumour, confirmed by x-ray mammography and detected on EIT images as white (high-conductive) area. The group 5 was created from group 4 by cutting out focus area from the images (13 partial EIM). Clinical diagnoses were affirmed by pre-surgery x-ray mammography and after-surgery patho-physiological macro- and micro- investigations. The average age of patients was 60 years; 50% of patients had arterial hypertension, 27% - oncological family inheritance.

Breast scanning was made at each 8 mm up to 6 cm depth (seven scanning planes). Wet gauze doilies were placed between breast skin and electrodes array to improve electric contact. Duration of one patient examination (preparation, carrying out measurements, image reconstruction and processing) was about 15-20 min. The analysis of EIM included: visual estimation of image at different scanning depth (searching for cancer symptomatic, determination of local conductivity); image filtering and calculating generalised characteristics of conductivity and its variability (average, standard deviation, max and min values); presentation of image as frequency distribution of conductivity (histogram) and comparison of frequency distribution at healthy and ill breast tissues using non-parametric analysis of difference (Kolmogorov-Smirnov criteria).

4. Results

4.1. Breast images

For correct estimation we compared mammograms obtained from the same scanning plane. With increasing scanning depth the scanning area of breast is decreased due to limited initial data. Note, that at all images given in this paper, the peripheral area, especially corners, is the region with bad contacts, and peripheral dark contours are artefacts related with transition from good to bad contacts. So reader should consider only central region inside these contours as region of interest.

Intact breast image (Figure 5) is characterized by absence of focal symptomatic, gray scale variety, smooth changing of conductivity ("mosaic"). These characteristics are kept at all scanning planes. Breast cancer EIM (Figure 6) is characterized by focal symptomatic as clear-cut light area of high conductivity and prevalence of dark tones contours of low conductivity. In our examinations the focus size varied from 2.0x0.8 cm up to 3.2x3.0 cm, spreading to the depth up to 3 cm.

4.2. Statistics

During analysis of EIM images obtained from the BCDD device, the tumours (focal alterations on the images) were visualised in 14 examinations (from total 21) - 67%. Another 4 EIM without clear focuses were estimated as abnormal due to conductivity distribution different from the typical distribution in normal breast (too poor gradations). As the result 86% of examinations were found fully or partially consistent with results of diagnostics by other methods. The causes of data mismatch were the following: hypermastia hampers examination due to limited scanning depth; some BCDD examinations were fulfilled after medical treatment (puncture, biopsy, x-ray therapy), which influenced the EIM.

Tissue conductivity is calculated in conventional units. Collection of average conductivity of intact and ill breasts at all scanning planes has a normal distribution. At first (nearest to the surface) plane, for example, the mean value $\mu = 0.89$ and standard deviation $\delta = 0.034$.

Average breast conductivity and standard deviations for groups 1 and 2 at different scanning planes are given in Table 1. The systematic decrease of conductivity with depth is the feature of the reconstruction software. It should be improved during further development by choosing more correct weighting coefficients at back projection procedure. Statistically significant differences in average conductivity between groups were not detected.

Table 1. Average breast conductivity in group 1 and group 2.

	1 scanning plane (0.4 cm)	3 scanning plane (2.0 cm)	5 scanning plane (3.6 cm)
Intact breast	0.89 ± 0.028	0.77 ± 0.056	0.68 ± 0.058
Cancer	0.88 ± 0.042	0.76 ± 0.077	0.69 ± 0.066

According to obtained EIM, the second group was divided into group 3 - 16 EIM without focal alterations and group 4 - 26 EIM with focal alterations. Group 5 – 13 partial EIM was created from group 4 by choosing focal area from entire images (EIM obtained from only one position – lying or standing, according to image quality, were used in this case). Average breast tissues conductivities in these groups are presented in Table 2.

Table 2. Average breast conductivity after subdividing of group 2.

	1 scanning plane(0.4 cm)	3 scanning plane (2.0 cm)	5 scanning plane (3.6 cm)
Group 1	0.89 ± 0.028	0.77 ± 0.056	0.68 ± 0.058
Group 3	0.86 ± 0.026	0.72 ± 0.049	0.66 ± 0.053
Group 4	0.91 ± 0.037	0.81 ± 0.066	0.70 ± 0.067
Group 5	0.99 ± 0.038	0.97 ± 0.067	0.96 ± 0.026

Using variance analysis we have found that differences between averages of groups for all scanning planes are statistically significant. With multiple comparison method - Newman-Keils criterion (Glantz 1994) we have shown up that averages of all groups at scanning plane 1

and 3 significantly differ from each other. At 5th scanning plane averages don't differ significantly due to lack of data.

4.3. Conductivity distribution on EIM

To compare images more accurately we used the histograms - graphic representation of images as frequency distribution of conductivity. To obtain reference distribution we have built the average diagram of frequency distribution of conductivity for intact breasts (average histogram). The obtained histogram, which we name "norm", is close to Gaussian distribution. Then we compared this average histogram with histograms of each EIM in 2, 3 and 4 groups.

For estimation of difference of conductivity distribution between norm (average histogram of group 1) and each EIM from groups 3 and 4 (as, for example, on Figure 7) we used the concept of distributions difference value (D_x). The calculation of D_x was carried out through Kholmogorov-Smirnov algorithm (see, for example, Gubler 1978). According to Gubler high significance of symptom is observed with distributions difference value 35-50%. We assume $D_x = 40\%$ as a point of separation of distributions and have found that for group 3 and group 4 90% of EIM diagrams (19 of 21) have significant (greater than separation point) difference with norm.

5. Discussion

The first experiments have demonstrated that a one-frequency static imaging EIT system with 256 electrodes, arranged in a two-dimensional matrix, is capable of producing images usable in breast cancer detection. The breast is the complex alveolar-tubular gland and consists of 15-20 lobules, which are encircled by adipose tissue. Complicated anatomic structure of breast tissues explains "mosaic" electrical impedance image of healthy breast. Appearance of focal alterations at EIM as clear-cut light areas is related with local conductivity increasing, which is common for tumours, much vascularised usually. Such focal alterations on EIT images were found at 67% of patients with breast cancer.

Analysis of average conductivity of breast tissues has shown that in groups 1, 3, 4 and 5 it differs significantly at all scanning planes. Pathologic focus (group 5) is distinguished by sharply increased conductivity kept at all scanning planes. Decreasing of average conductivity of breast tissues in group 3 can be related with changing of electrical characteristics after x-ray medical treatment or background state preceding the tumour appearance.

We have found that with the increasing scanning depth in groups 3 and 4 the percentage of multi-modal distributions increased. Asymmetry and distributions shifts in comparison with norm in these groups have various directions. Therefore in order to determine the value of conductivity distributions difference in 1, 2, 3 and 4 groups it is necessary to use non-parametric criterions. The developed approach for the estimation the difference of conductivity distributions based on Kholmogorov-Smirnov criterion seems useable in population screening examinations. Investigations involving a larger number of patients and taking into account the menstrual cycle, presence of cysts and other non-cancerous formations in breast tissue should be continued to get more reliable data.

Acknowledgement

This work was supported by Technology Commercialization International, Inc., 1650 University Blvd. NE, Albuquerque, New Mexico, 87102, USA as part of the TCInternational Breast Cancer Detection Device program.

References

Cherepenin V A, Korjenevsky A V, Kornienko V N, Kultiasov M Y, Kultiasov Y S 1995 The electrical impedance tomograph: new capabilities *Proc. 9th Int. Conf. On Electrical Bio-Impedance (Heidelberg, 1995)* 430-33

Glantz S A 1994 *Primer of biostatistics* (McGraw-Hill)

Gubler E 1978 *Calculation methods of analysis and recognition of pathological processes* (Leningrad: Meditsina)

Korjenevsky A V 1995 Reconstruction of absolute conductivity distribution in electrical impedance tomography *Proc. 9th Int. Conf. On Electrical Bio-Impedance (Heidelberg, 1995)* 532-35

Korjenevsky A V, Kornienko V N, Kultiasov M Y, Kultiasov Y S and Cherepenin V A 1997 *Pribory i Tekhnika Experimenta* No 3 133-40 (Engl. transl. Korzhenevskii A V, Kornienko V N, Kul'tiasov M Y, Kul'tiasov Y S and Cherepenin V A Electrical impedance computerized tomograph for medical applications *Instruments and Experimental Techniques* **40** 415-21)

Rigaud B, Morucci J P and Chauveau N 1996 Bioelectrical impedance techniques in medicine Part I: Bioimpedance measurements Second Section: impedance spectrometry *Crit. Rev. Biomed. Eng.* **24** 257-351

Tunstall B, Wang W, Cheng Z, McCormik M, Walker R and Rew D 1998 In-vitro study results from De Montfort Mk1 electrical impedance mammography system *Proc. 10th Int. Conf. On Electrical Bio-Impedance (Barcelona, 1998)* 525-28

Wtorek J, Stelter J and Nowakowski A 1999 Impedance mammograph 3D phantom studies *Ann. NY Acad. Sci.* **873** 520-33

FIGURE CAPTIONS

Figure 1. Physical configuration of the system and measuring procedure: 1 - plane with 256 electrodes, 2 - grips with remote electrodes.

Figure 2. Realisation of 3D visualisation.

Figure 3. Imaging of the cylindrical glass immersed vertically into the tank with saline.

Figure 4. Male breast images (first 3 cross-sections): 1 – nipple, 2 – ribs, 3 – zone, corresponding to boundary between good and fault contacts on the plane with electrodes.

Figure 5. EIM image of intact breast at 1.2-cm depth.

Figure 6. EIM image of breast cancer at 1.2-cm scanning plane; the cancer area is above and to the left from the centre of image.

Figure 7. Comparison of EIM histograms: 1 – average histogram of impact breast images (norm), 2 – one of the histograms for the breast with cancer; the D_x parameter is 51% for these two distributions.

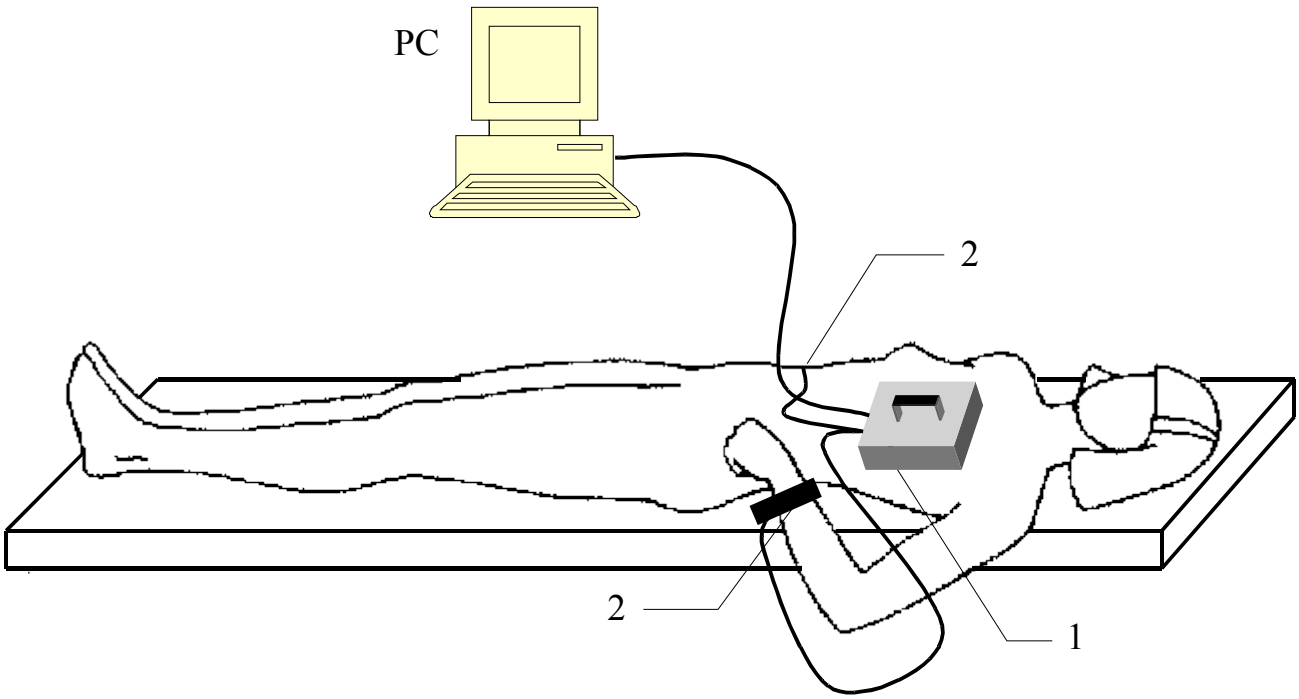

Figure 1.

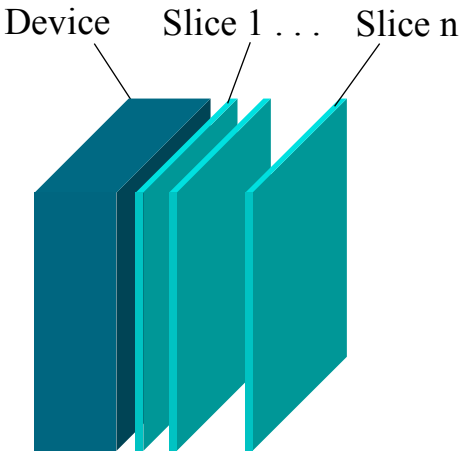

Figure 2.

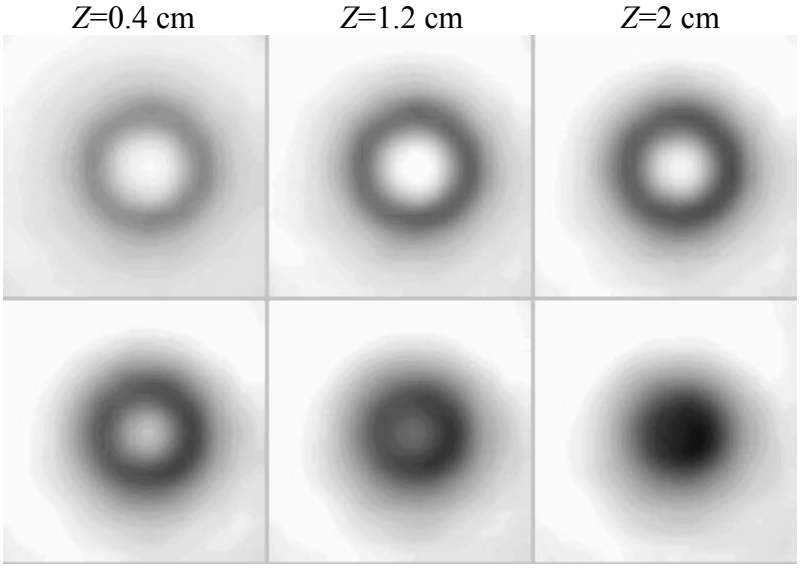

Figure 3.

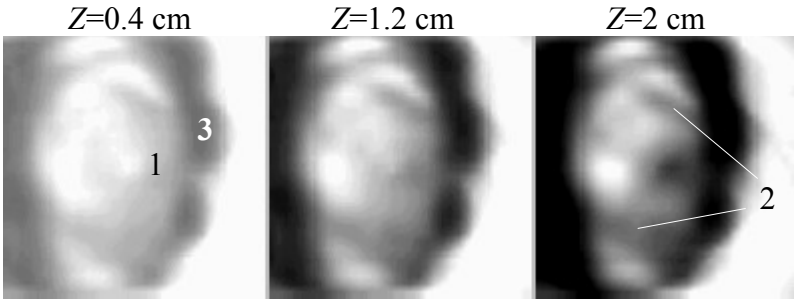

Figure 4.

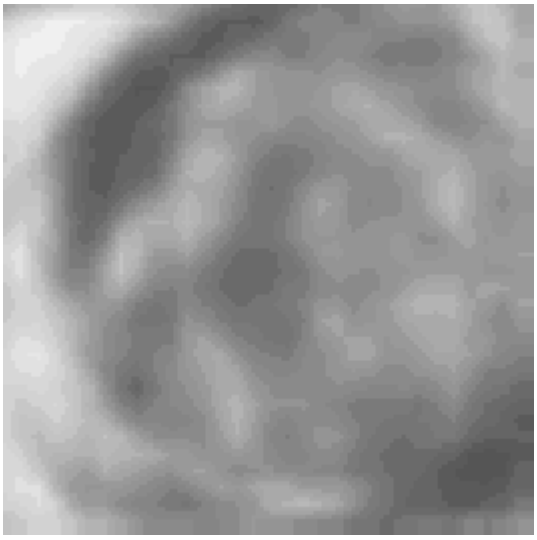

Figure 5.

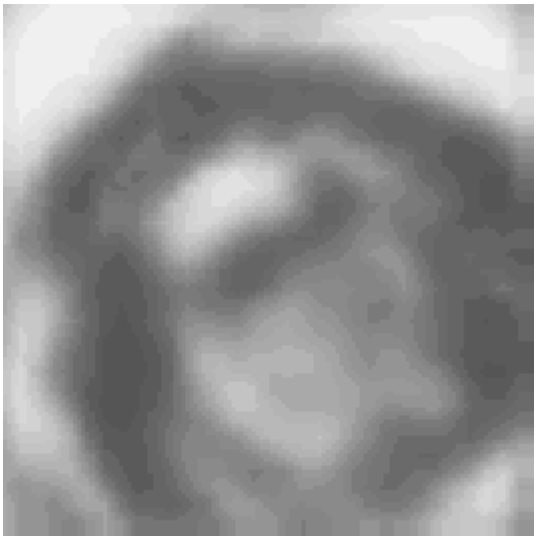

Figure 6.

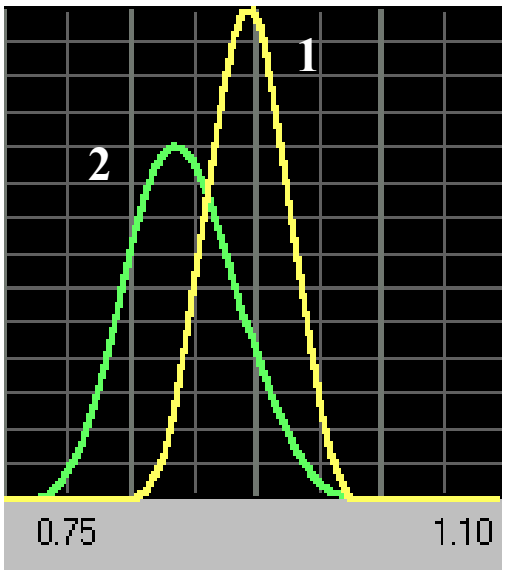

Figure 7.